

ENGINEERING DESIGN AND PROTOTYPE FABRICATION OF HOM COUPLERS FOR HL-LHC CRAB CAVITIES *

C. Zanoni^{†1}, S. Atieh¹, I. Aviles Santillana^{1,2}, S. Belomestnykh^{3,4}, G. Burt⁵, R. Calaga¹, O. Capatina¹, T. Capelli¹, F. Carra¹, S.U. De Silva⁶, J. Delayan⁶, P. Freijedo Menendez¹, M. Garlaschè¹, J.-M. Geisser¹, T. Jones⁷, R. Leuxe¹, Z. Li⁸, L. Marques Antunes Ferreira¹, A. May⁷, T. Nicol⁹, R. Olave⁶, H. Park⁶, S. Patalwar⁷, A. Ratti¹⁰, E. Rigutto¹, N. Templeton⁷, S. Verdu-Andres³, Q. Wu³, and B. Xiao³

¹CERN, Geneva, Switzerland

²University Carlos III, 28911 Madrid, Spain

³BNL, Upton, NY 11973, USA

⁴Stony Brook University, Stony Brook, NY 11794, USA

⁵Cockcroft Institute, Lancaster University, UK

⁶Old Dominion University, Norfolk, VA, 23529, USA

⁷STFC Daresbury Laboratory, UK

⁸SLAC, Menlo Park, CA 94025, USA

⁹Fermilab, Batavia, IL 60510, USA

¹⁰LBNL, Berkeley, CA 94707, USA

Abstract

The HL-LHC upgrade relies on a set of RF crab cavities for reaching its goals. Two parallel concepts, the Double Quarter Wave (DQW) and the RF Dipole (RFD), are going through a comprehensive design process along with preparation of fabrication in view of extensive tests with beam in SPS. High Order Modes (HOM) couplers are critical in providing damping in RF cavities during operation in accelerators. HOM prototyping and fabrication have recently started at CERN.

In this paper, an overview of the final geometry is provided along with an insight in the mechanical and thermal analyses performed to validate the design of this critical component. Emphasis is also given to material selection, prototyping, initial fabrication and test campaigns that are aimed at fulfilling the highly demanding tolerances of the couplers.

Two parallel concepts for such cavities are under development: the Double Quarter Wave (DQW) and the RF Dipole (RFD). In the scope of these cavities, so called High Order Modes (HOM) couplers are also under design [2, 3], prototyping and fabrication.

The coupler is needed for damping detrimental modes with frequencies higher than the fundamental one. Such modes, induced by the passage of the charged beam in the cavity, have profound consequences in terms of power dissipation and stability of the beam [4]. Each DQW cavity needs 3 HOM couplers. The RFD have 2 HOM couplers each in 2 variants.

The geometry of the DQW and RFD HOM couplers are depicted in Figure 1. This paper overviews the thermo-mechanical assessment and early fabrication of these systems. Other aspects of the cavity design and engineering are treated elsewhere in this conference [5–7].

INTRODUCTION

The statistical gain obtained by running LHC after 2020 with the current performance is marginal [1]. Thus, in order to keep LHC at the forefront of physics, a significant luminosity increase is foreseen through the HL-LHC (High Luminosity LHC) upgrade. The crab cavities are among the critical systems required for obtaining the desired new performance. They compensate the bunch crossing angle, and thus maximize the integrated luminosity and provide instant luminosity leveling.

* The research leading to these results has received funding from the European Commission under the FP7 project HiLumi LHC, GA no. 284404, co-funded by the DoE, USA and KEK, Japan

[†] carlo.zanoni@cern.ch

ASSESSMENT OF THE MECHANICAL PERFORMANCE

The DQW HOM coupler is made of a niobium shell that continues the cavity envelope and supports a hook. The hook performs the extraction of the high frequency electromagnetic modes. The external shell is in AISI 316LN (stainless steel) that contains the superfluid cryogenic helium during operation. The 316LN jacket also includes bellows that limit the effect of deformations due to welding.

The heat deposition in the hook due to the RF electromagnetic field is in the order of 17 mW. The coupler is actively cooled in order to cope with tolerances (0.1 mm shape error can determine up to 0.1 W extra load) and minimize temper-

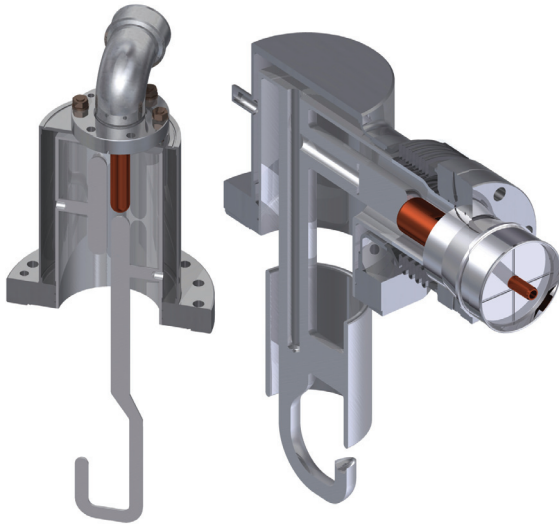


Figure 1: View of the RFD (left) and DQW (right) HOMs.

ature increase due to the static and dynamic load from the RF line.

The properties of the chosen materials are in Table 1, where both the value at room temperature and at 2K are shown.

The performance of the HOM are analyzed according to the following constraints:

1. the stress must comply with the materials yield strengths with an adequate safety factor;
2. the displacement of the HOM hook with respect to the surrounding tube, must be small enough to avoid significant changes in the RF performance;
3. the 1st mechanical mode should be sufficiently high.

Main Assumptions and Load Cases

The analysis of the mechanical performance is mainly performed in ANSYS15 and relies on the following assumptions:

- the vacuum brazing between 316LN and niobium in the flanges are not modeled, as such an effort alone would be too demanding. However, such a brazing is common at CERN;
- the temperature is uniform all over the object;
- the Elastic modulus and Poisson's ratio are the same at 2 K and 300 K;
- the HOM lines do not apply any constraint on the vertical flange. The same applies to the lines that feed helium between 316LN and niobium parts.

The HOM model is assumed constrained only at the horizontal flange. In practice, the bolt holes are constrained to a null remote displacement and rotation with respect to the flange center, i.e. the average value of all the nodes is fixed,

not the single nodal value. The remote displacement is chosen because it allows a deformable boundary condition and therefore model thermal contraction.

Three load cases are analyzed:

1. $T = 2 \text{ K}$, $p = 0.18 \text{ MPa}$ (absolute), gravity. This is the status of the HOM towards the end of cool down. The different contraction coefficient between 316LN and niobium induces significant loads. On the other hand, at cryo temperature, the allowable stress of materials is higher;
2. $T = 300 \text{ K}$, $p = 0.18 \text{ MPa}$ (absolute), gravity. This is the status of the HOM at the beginning of cool down;
3. $T = 2 \text{ K}$, $p = 0 \text{ MPa}$, gravity. This is the load condition during normal operation.

For all these cases, the presence of gravity means that there is also a load coming from the RF connecting line on the vertical flange. Such a weight is modeled as a remote force of 50 N with a lever-arm of about 760 mm¹. All these values are taken with a margin (overall it is more than 2.5) that accounts for possible unexpected loads during assembly, mounting and transport. In the load cases in which the thermal contraction is not applied, the remote displacement is substituted with a fixed support.

Figure 2 shows the configuration of the electron-beam welds performed on 316LN. The circular welds are performed with niobium already inside. In order to avoid issues, a small protective 316LN surface is included that intercepts and absorbs any electron that would hit niobium. This makes indeed easier and safer the welding process, but adds some complexity in the assessment phase. Full penetration welds are standard and are verified as any other part of bulk material.

The reduction in cross section implies a concentration of stresses. The effect of a sharp angle is hard to be analyzed with a linear elastic FE calculation. An elasto-plastic model is indeed feasible, but it would be computationally heavy and not necessarily justified. The peak values are therefore initially assessed. The mesh in all the welds has a fixed dimension that is controlled and gradually reduced. The peak value grows with the decrease in mesh dimension. The weld is then assessed accordingly. It is worth noting that the couplers are not subject to fatigue, therefore localized peaks are not of concern.

Results and Welds Qualification

The stress intensity all over the HOM is compared with the relevant material properties, Table 1.

Figure 3 shows the stress in niobium at 300 K and 0.18 MPa of pressure. One issue in evaluating the results is that the stress is locally very high where the flanges are brazed. In fact, the copper layer between niobium and 316LN is

¹ if a coordinate system is put in the flange with z as axis of the flange internal cylinder and y aligned with gravity: 300 mm of distance in x, 700 mm in z

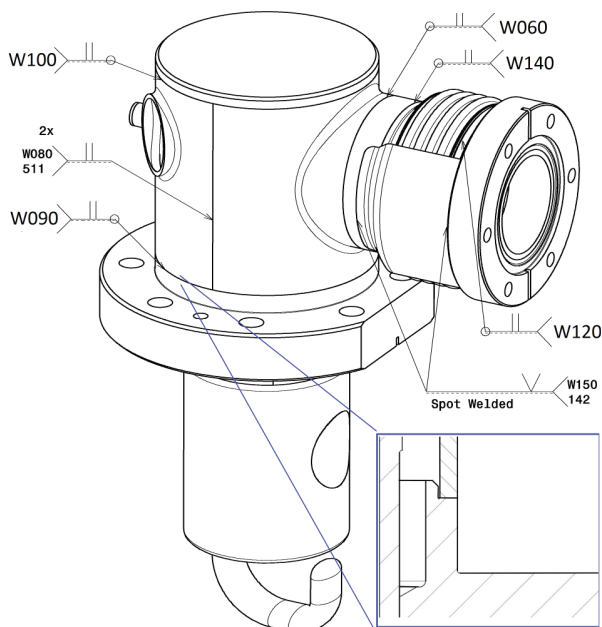


Figure 2: Configuration of the welds. The EBW code (511) is omitted in the critical welds, for clarity of the picture.

Table 1: Material Properties [8–11]

		300 K	2 K
Nb	$Rp_{0.2}$ [MPa]	75	480
	$Rp_{0.2}/1.5$ [MPa]	50	320
316LN	$Rp_{0.2}$ [MPa]	280	821
	$Rp_{0.2}/1.5$ [MPa]	187	547

not modeled and there is a sharp edge in contact. If the localized effects due to contacts and non-modeled items are neglected, the most demanding condition is at the elbow for both materials. Table 2 summarizes the stress intensities in those locations. Those values are compared with the allowable stress of Table 1 divide by 1.5 as indicated in the pressure equipment standard [12].

Table 2: Peak Stress Intensities at the Elbow

	Temperature	Stress [MPa]
Nb	2K	80
	300K	28
316LN	2K	170
	300K	27

Table 3: Peak Stress at the Welds (2 K)

Peak at 2 K [MPa], Allowable stress: 547 MPa				
mesh [mm]	1	0.5	0.3	0.1
W090	121	132	156	190
W060	230	242	296	402
W140	124	122	112	139
W100	189	205	236	338
W120	53	56	64	76

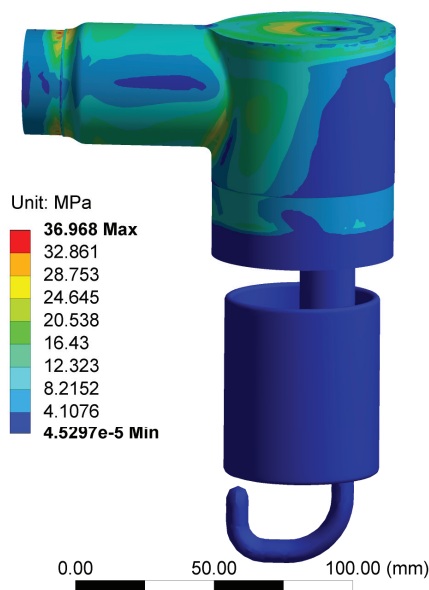


Figure 3: Stress intensity in niobium at 300 K and 0.18 MPa of pressure.

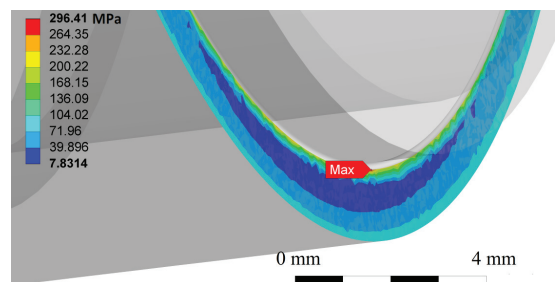


Figure 4: Stress peak in weld W060 with mesh elements 0.3 mm.

Table 4: Peak Stress at the Welds (300 K)

Peak at 300 K [MPa], Allowable stress: 187 MPa				
mesh [mm]	1	0.5	0.3	0.1
W090	23	26	31	37
W060	31	34	43	55
W140	21	18	19	26
W100	62	76	81	115
W120	15	15	18	22

Tables 3 and 4 show the value of the peak stress in the welds as a function of the mesh at both 300K and 2K. Figure 4 shows an example of local stress. Even with an element size of 0.1 mm, the peak is below the elastic limit. Further reduction in mesh size is not justified and it is assumed that if there is a plasticization it will be extremely localized. Taking into account the absence of any fatigue load, the welds can be considered safe.

FABRICATION STRATEGY AND RESULTS

RF requirements in terms of final geometry and position tolerances for the DQW and RFD HOM assemblies range in the order of few tenths of mm ($0.2 \text{ mm} \div 0.5 \text{ mm}$). In order to comply with such requirements, the HOM assemblies are divided into the minimum number of subcomponents – so to minimize joining steps - while still trying to maximize simplicity of fabrication. Figure 5 shows an exploded view of the DQW HOM, which is currently under pre-series fabrication at CERN shortly to be followed by the RFD HOM couplers.

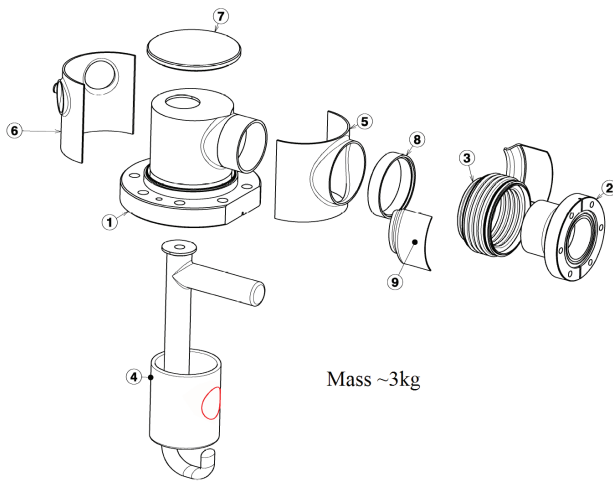


Figure 5: Exploded view of the DQW HOM.

As shown in Figure 5 the overall assembly is composed of 13 sub-elements; the path from such sub-components to the complete assembly foresees not less than 30 fabrication steps, merging different technologies: from precise machining to joining, chemical and thermal treatments. Together with the tight tolerance requirements, this adds to the complexity of the fabrication of such critical pieces.

Machining

All main niobium subcomponents are obtained via material removal from bulk material. This allows a reduction in the number of inclusions with respect to sheet raw material and corresponding fabrication processes (e.g. drawing, forming).

Precise machining of the geometrically-exotic niobium parts is performed on a 5 axis milling center (see hook in Figure 6). Current fabrication of such part yields to profile errors in the order of $\pm 10 \mu\text{m}$; such values are well below specified tolerances but become a hard requirement when accounting for further error contributions during the subsequent assembly steps. The remaining parts call for more standard fabrication approaches, but still entail precise tolerance output.

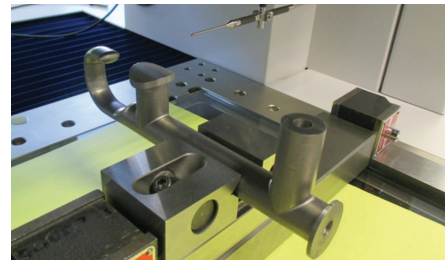


Figure 6: CMM metrology of niobium hook at CERN.

Joining Processes

For positions 1 and 2 in Figure 5, a direct brazing of niobium tubes to 316LN flanges is chosen. Such procedure was developed at CERN in the framework of the LEP accelerator [13] and successfully implemented in other projects such as SPL [14].

All other joining steps foresee the implementation of electron beam welding. This is the process of choice when there is the need to maintain cryogenic requirements for niobium and to comply with strict RF requirements in terms of weld non-conformities. The position and geometry of the welds, which favor full-penetration weld configurations, have been chosen in order to comply with cryogenic vessel normative and allow the highest number of non destructive checks.

Electron beam welding is also the current baseline for realization of the 316LN welds. Thus minimizes deformations and possible damages to the niobium parts.

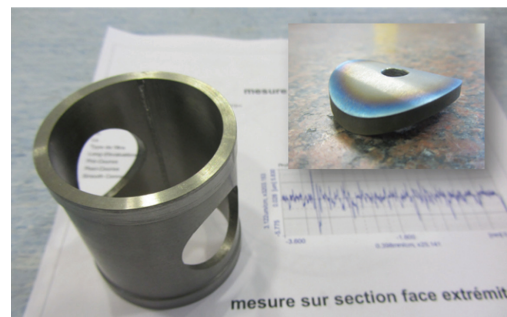


Figure 7: Welded specimens for qualification of the full-penetration weld between the hook and the niobium corona.

Figure 7 shows the welded specimens for qualification of the butt-weld between the hook and the niobium corona (red in Figure 5). Such weld is critical due to its position on the HOM and to the varying thickness of the interfaces to be joined. Despite its complexity, such configuration is chosen to facilitate the 3-dimensional machining of the hook itself.

Surface Treatment

In order to prepare niobium surfaces for RF, an etching of such surfaces is performed (Buffered Chemical Polishing, BCP). The specified amount of thickness to be etched away varies for the different HOMs, ranging between $50 \mu\text{m}$ and $100 \mu\text{m}$. Thanks to the implementation of machining from

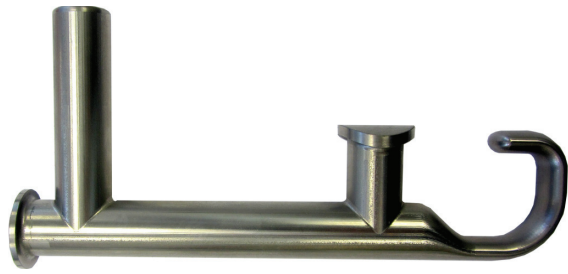


Figure 8: Fabricated DQW HOM hook.

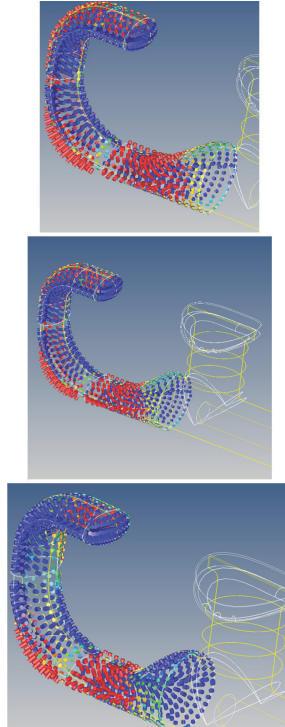


Figure 9: From top to bottom: dimensional control before any BCP, after the first step (20 μm theoretical removal) and the second step (31 μm theoretical removal). Red is a deviation from nominal geometry of +10 μm , blue is -10 μm .

solid niobium bulks, such thickness is reduced with respect to usual requirements for formed-sheet pieces, where size of foreign material inclusions is much more developed.

Since the BCP results highly depend on geometry and specific process parameters, the first prototype of the DQW HOM hook has been devoted to qualification BCP erosion. Dimensional controls after multiple BCP steps, show that resulting etched thickness is sufficiently coherent with the sought values, Figure 9: a variability around $\pm 10 \mu\text{m}$ with respect to the theoretical value is obtained. This is already acceptable in terms of tolerances required; furthermore the results from the BCP campaign on the first prototype will be useful for validation of the final pre-BCP geometry. Figure 8 shows one of the first fabricated hooks, after prototyping.

CONCLUSIONS

Stability of the beam and power dissipation are strongly influenced by High Order Modes in cavities. In order to control such modes, HOM couplers are needed in all RF cavities. In the frame of the HL-LHC upgrade and the development of the compact crab cavities, HOM couplers were developed both in terms of RF and thermo-mechanical performance and are on-going fabrication.

Fabrication of the HOM couplers entails challenging solutions and complex multidisciplinary approaches. Nonetheless, the tests following the first fabrication steps are very encouraging.

REFERENCES

- [1] G. Apollinari, O. Brüning and L. Rossi, "High Luminosity LHC Project Description", CERN-ACC-2014-0321, Geneva (2014), <http://cds.cern.ch/record/1974419>
- [2] Zenghai Li et al., "FPC and Hi-Pass Filter HOM Coupler Design for the RF Dipole Crab Cavity for the LHC High Luminosity Upgrade," WEPWI004, IPAC'15, Richmond, USA (2015).
- [3] B. Xiao et al., "Higher Order Mode Filter Design for Double Quarter Wave Crab Cavity for the LHC High Luminosity Upgrade," WEPWI004, IPAC'15, Richmond, USA (2015).
- [4] H. Padamsee, *RF Superconductivity: Science, Technology, and Applications*, 2nd ed., Wiley, New York, USA (2009).
- [5] C. Zanoni et al., "Design of Dressed Crab Cavities for the HL-LHC Upgrade," THPB070, *these proceedings*, SRF'15, Whistler, Canada (2015).
- [6] K. Artoos et al., "Development of SRF Cavity Tuners for CERN," THPB060, *these proceedings*, SRF'15, Whistler, Canada (2015).
- [7] F. Carra et al., "Crab Cavity and Cryomodule Development for HL-LHC," FRBA02, *these proceedings*, SRF'15, Whistler, Canada (2015).
- [8] "Material Technical Specification N° 3300. Pure niobium sheets, grade RRR300," CERN internal document, EDMS 1095252 (2015).
- [9] "Dressed Niobium SRF Cavity Pressure Safety," FermiLab document, FESHM Chapter 5031.6., ESHQ 1097-v4 (2014).
- [10] "EN 10028-7:2008, Flat products made of steels for pressure purposes Part 7: Stainless steels," Paris, France (2008).
- [11] A. Gerardin, "Tensile tests on CS conductor jackets, samples 22bis and sample XX," CERN internal document, EDMS 1086500 (2010).
- [12] VV.AA., "EN 13445-3", Paris, France (2008).
- [13] J.P. Bacher, E. Chiaveri and B. Trincat, "Brazing of niobium to stainless steel for UHV applications in superconducting cavities," CERN internal document, CERN-EF-RF-87-7 (1987), <http://cds.cern.ch/record/948207>
- [14] N.V. Valverde Alonso et al., "Electron Beam Welding and Vacuum Brazing Characterization for SRF Cavities," THPP039, Proceedings of LINAC2014 (2014).